2D DUAL-TREE M-BAND WAVELET DECOMPOSITION

Caroline Chaux[1], Laurent Duval[2] and Jean-Christophe Pesquet[1]

[1]Institut Gaspard Monge and UMR-CNRS 8049
Université de Marne-la-Vallée, Champs-sur-Marne
77454 Marne-la-Vallée, France
e-mail: {chaux,pesquet}@univ-mlv.fr

[2] Institut Français du Pétrole
Technology, Comp. Sci. and Appl. Math. Dpt.
92500 Rueil Malmaison, France
e-mail : laurent.duval@ifp.fr

ABSTRACT

We propose a 2D generalization to the M-band case of the dual-tree structure (initially proposed by N. Kingsbury and further investigated by I. Selesnick) based on a Hilbert pair of wavelets. We particularly address the construction of the dual basis and the resulting directional analysis. We revisit the necessary pre-processing stage in the M-band case. While several reconstructions are possible because of the redundancy of the representation, we propose a new optimal signal reconstruction technique, which minimizes potential estimation errors. The effectiveness of the proposed M-band decomposition is demonstrated via image denoising comparisons.

1. INTRODUCTION

The classical discrete wavelet transform (DWT) provides a means of implementing a multiscale analysis, based on a critically sampled filter bank with perfect reconstruction. It has shown very effective both theoretically and practically [1] in the processing of certain classes of signals, for instance piecewise smooth signals, having a finite number of discontinuities. But, while decimated transforms yield good compression performance, other data processing applications (denoising, analysis, detection) often require other schemes, mitigating three of the typical DWT weaknesses.

One first drawback usually limits the practical performance of DWT algorithms: (I) shift-variance, with respect to the value of the transformed coefficients at a given scale. It often results in shift-variant edge artifacts at the vicinity of jumps, which are not desirable in real-world applications, signal delay being rarely known. A second drawback arises in dimensions higher than 1: tensor products of classical wavelets usually possess (II) poor directional properties. The later problem is sensitive in image detection or denoising applications.

A vast majority of the proposed solutions relies on adding some redundancy to the transform. Redundancy based on shift-invariant wavelet transforms [2] suppresses shift dependencies, at the expense of an increased computational cost, which often becomes intractable in higher dimensions. Less computationally-expensive approaches have been developed on complex filters for real signals (we refer to [3] for an overview and design examples), or by employing other wavelet frames [4]. For instance, it is possible to resort to the concatenation of several wavelet bases. One of the most promising decomposition is the *dual-tree* discrete wavelet transform, proposed by N. Kingsbury [5]: two classical wavelet trees are developed in parallel, with filters forming Hilbert pairs. Advantages of Hilbert pairs had been earlier recognized by other authors [6]. The resulting analysis yields a redundancy of only 2^d

for d-dimensional signals, with a much lower shift sensitivity and better directionality in 2D than the DWT.

The design of dual-tree filters is addressed in [7], through an approximate Hilbert pair formulation for the "dual" wavelets. I. Selesnick also proposed the double-density DWT and combined both frame approaches [8]. The *phaselet* extension of the dual-tree DWT has been recently introduced by R. Gopinath in [9].

More recently, several authors have also proposed a projection scheme with an explicit control of the redundancy or with specific filter bank structures [10, 11]. Finally, other works on the blending of analytic signals and wavelets must be mentioned [12, 13], in the context of denoising or higher dimension signal processing. Developments based on "geometrical" wavelets will not be mentioned here, in spite of their interest.

A third drawback, less frequently pointed out, concerns (III) design limitations in two-band decompositions: orthogonality, realness, symmetry, compactness of the support and other properties (regularity, vanishing moments) compete. The relative sparsity of good filter banks amongst all possible solutions is also well-known. In order to improve both design freedom and filter behavior, M-band filter banks and wavelets have been proposed [14–16].

Improving on our previous work [17], we propose the construction of a 2D dual-tree M-band wavelet decomposition. The organization of the paper is as follow: in Section 2, we review the theory for the construction of M-band Hilbert pairs. In Section 3, we extend previous results on the pre-processing stage to the M-band context and illustrate the direction extraction with the constructed wavelets. Since several reconstructions are possible, due to the decomposition redundancy, Section 4 then proposes an optimal pseudo-inverse based frame reconstruction, which allows to reduce the effects of coefficient estimation errors. Finally, we provide practical results for image denoising applications in Section 5. Conclusions are drawn in Section 6.

2. CONSTRUCTION OF M-BAND HILBERT PAIRS

In this section, we will focus on 1D signals belonging to the space $L^2(\mathbb{R})$. Recall that an M-band multiresolution analysis of $L^2(\mathbb{R})$ (with $M \geq 2$) is defined by one scaling function (or father wavelet) $\psi_0 \in L^2(\mathbb{R})$ and $(M-1)$ mother wavelets $\psi_m \in L^2(\mathbb{R})$, $m \in \{1, \ldots, M-1\}$ [15]. These functions are solutions of the following scaling equations:

$$\frac{1}{\sqrt{M}}\psi_m(\frac{t}{M}) = \sum_{k=-\infty}^{\infty} h_m[k]\psi_0(t-k), \qquad (1)$$

where the sequences $(h_m[k])_{k\in\mathbb{Z}}$ are square summable. In the following, we will assume that these functions (and thus the associ-

ated sequences $(h_m[k])_{k\in\mathbb{Z}}$ are real-valued. The Fourier transform of $(h_m[k])_{k\in\mathbb{Z}}$ is a 2π-periodic function, denoted by H_m. For the set of functions $\cup_{m=1}^{M-1}\{M^{-j/2}\psi_m(M^{-j}t-k),(j,k)\in\mathbb{Z}^2\}$ to correspond to an orthonormal basis of $L^2(\mathbb{R})$, the following para-unitarity conditions must hold:

$$\sum_{p=0}^{M-1}H_m(\omega+p\frac{2\pi}{M})H_{m'}^*(\omega+p\frac{2\pi}{M})=M\delta_{m-m'},\qquad(2)$$

where $\delta_m=1$ if $m=0$ and 0 otherwise.

Our objective is to construct a "dual" M-band multiresolution analysis defined by a scaling function ψ_0^{H} and mother wavelets ψ_m^{H}, $m\in\{1,\ldots,M-1\}$. More precisely, the mother wavelets will be obtained by a Hilbert transform from the "original" wavelets ψ_m, $m\in\{1,\ldots,M-1\}$. In the Fourier domain, the desired property reads:

$$\forall m\in\{1,\ldots,M-1\},\qquad\widehat{\psi}_m^{\mathrm{H}}(\omega)=-\imath\,\mathrm{sign}(\omega)\widehat{\psi}_m(\omega),\ \ (3)$$

where sign is the signum function and $\widehat{a}$ designates the Fourier transform of a function a. Furthermore, the functions ψ_m^{H} are defined by scaling equations similar to (1) involving real-valued sequences $(g_m[k])_{k\in\mathbb{Z}}$. In order to generate a dual M-band orthonormal wavelet basis of $L^2(\mathbb{R})$, the Fourier transforms G_m of the sequences $(g_m[k])_{k\in\mathbb{Z}}$ must also satisfy para-unitarity conditions.

The Hilbert condition (3) yields:

$$\forall m\in\{1,\ldots,M-1\},\qquad|\widehat{\psi}_m^{\mathrm{H}}(\omega)|=|\widehat{\psi}_m(\omega)|.\quad(4)$$

If we further impose that $|\widehat{\psi}_0^{\mathrm{H}}(\omega)|=|\widehat{\psi}_0(\omega)|$, the scaling equations lead to:

$$\forall m\in\{0,\ldots,M-1\},\qquad G_m(\omega)=e^{-\imath\theta_m(\omega)}H_m(\omega),\ \ (5)$$

where θ_m is 2π-periodic. The frequency phase functions should also be odd (for real filters) and thus only need to be determined over $[0,\pi]$.

In the 2-band case (under weak assumptions), θ_0 is a linear function on $[-\pi,\pi[$ [7]. In the M-band case, we will slightly restrict this constraint on a smaller interval by imposing: $\forall\omega\in[0,2\pi/M[$, $\theta_0(\omega)=\gamma\omega$, where $\gamma\in\mathbb{R}$. Then, after some tedious calculations [17], the following result can be proved:

Proposition 1 *Para-unitary M-band Hilbert filter banks are obtained by choosing the phase functions defined by:*

$$\forall p\in\left\{0,\ldots,\left\lceil\frac{M}{2}\right\rceil-1\right\},\forall\omega\in\left[p\frac{2\pi}{M},(p+1)\frac{2\pi}{M}\right[,$$

$$\theta_0(\omega)=(d+\frac{1}{2})(M-1)\,\omega-p\pi,$$

$$\forall m\in\{1,\ldots,M-1\},$$

$$\theta_m(\omega)=\begin{cases}\dfrac{\pi}{2}-(d+\dfrac{1}{2})\omega & \text{if }\omega\in]0,2\pi[,\\0 & \text{if }\omega=0,\end{cases}$$

where $d\in\mathbb{Z}$ and $\lceil u\rceil$ denotes the upper integer part of a real u. The scaling function associated to the dual wavelet decomposition is such that:

$$\forall k\in\mathbb{N},\ \forall\omega\in[2k\pi,2(k+1)\pi[,$$
$$\widehat{\psi}_0^{\mathrm{H}}(\omega)=(-1)^k e^{-\imath(d+\frac{1}{2})\omega}\,\widehat{\psi}_0(\omega).\quad(6)$$

It should also be noted that, except in the 2-band case, θ_0 exhibits discontinuities on $]0,\pi[$, due to the $p\pi$ term.

3. 2D DUAL-TREE DECOMPOSITION

Two-dimensional separable M-band wavelet bases can be derived from the 1D dual-tree decomposition. Thus, we obtain two bases of $L^2(\mathbb{R}^2)$: the first one corresponds to the classical 2D separable wavelet basis while the second one results from tensor products of the dual wavelet basis functions. A discrete implementation of these wavelet decompositions starts from level $j=1$ to go up to the coarsest resolution level $J\in\mathbb{N}^*$. The decomposition onto the former 2D wavelet basis yields coefficients $c_{j,m,m'}[k,l]$, whereas the decomposition onto the dual basis generates coefficients $c_{j,m,m'}^{\mathrm{H}}[k,l]$. As pointed out in the seminal works of Kingsbury and Selesnick, it is advantageous to add some pre- and post-processings to this decomposition. We will now revisit these problems in the context of M-band decompositions.

3.1. Prefiltering

The wavelet transform is a continuous-space formalism that we want to apply to a "discrete" image. We consider that the analog scene corresponds to the 2D field:

$$f(x,y)=\sum_{k,l}f[k,l]\,s(x-k,y-l),\qquad(7)$$

where s is some interpolation function and $(f[k,l])_{(k,l)\in\mathbb{Z}^2}$ is the image sample sequence. Let us project the image onto the approximation space $V_0=\overline{\mathrm{Span}}\{\psi_0(x-k)\psi_0(y-l),(k,l)\in\mathbb{Z}^2\}$. The projection of f reads:

$$P_{V_0}(f(x,y))=\sum_{k,l}c_{0,0,0}[k,l]\,\psi_0(x-k)\,\psi_0(y-l),\quad(8)$$

where the approximation coefficients are

$$c_{0,0,0}[k,l]=\langle f(x,y),\psi_0(x-k)\,\psi_0(y-l)\rangle,\qquad(9)$$

and $\langle\,,\,\rangle$ denotes the inner product of $L^2(\mathbb{R}^2)$. Using Eq. (7), we obtain:

$$c_{0,0,0}[k,l]=\sum_{p,q}f[p,q]\,\gamma_{s,\Psi_{0,0}}(k-p,l-q),\qquad(10)$$

where $\Psi_{0,0}(x,y)=\psi_0(x)\psi_0(y)$ and $\gamma_{s,\Psi_{0,0}}$ is the cross-correlation function defined as:

$$\gamma_{s,\Psi_{0,0}}(x,y)=\int_{-\infty}^{\infty}\int_{-\infty}^{\infty}s(u,v)\Psi_{0,0}(u-x,v-y)\,du\,dv.$$
$$(11)$$

Similarly, we can project the analog image onto the dual approximation space $V_0^{\mathrm{H}}=\overline{\mathrm{Span}}\{\Psi_{0,0}^{\mathrm{H}}(x-k,y-l),(k,l)\in\mathbb{Z}^2\}$ where $\Psi_{0,0}^{\mathrm{H}}(x,y)=\psi_0^{\mathrm{H}}(x)\psi_0^{\mathrm{H}}(y)$. Then, the dual approximation coefficients are given by:

$$c_{0,0,0}^{\mathrm{H}}[k,l]=\sum_{p,q}f[p,q]\,\gamma_{s,\Psi_{0,0}^{\mathrm{H}}}(k-p,l-q).\qquad(12)$$

Obviously, Eq. (10) and (12) can be interpreted as the use of two prefilters on the discrete image $(f[k,l])_{(k,l)\in\mathbb{Z}^2}$ before the dual-tree decomposition. The frequency responses of these filters are

$$F_1(\omega_x,\omega_y)=$$

$$\sum_{p=-\infty}^{\infty}\sum_{q=-\infty}^{\infty}\widehat{s}(\omega_x+2p\pi,\omega_y+2q\pi)\widehat{\psi}_0^*(\omega_x+2p\pi)\widehat{\psi}_0^*(\omega_y+2q\pi)$$

$$F_2(\omega_x,\omega_y)=e^{\imath(d+1/2)(\omega_x+\omega_y)}F_1(\omega_x,\omega_y).$$

Different kinds of interpolation functions may be considered, for instance separable functions of the form $s(x,y) = \chi(x)\chi(y)$. The two prefilters are then separable with impulse responses $\gamma_{\chi,\psi_0}(p)$ $\gamma_{\chi,\psi_0}(q)$ and $\gamma_{\chi,\psi_0^H}(p)\gamma_{\chi,\psi_0^H}(q)$, respectively. A possible choice for χ is the Shannon-Nyquist interpolation function, $\chi(t) = \mathrm{sinc}(\pi t)$, which allows ideal digital-to-analog conversion of a band-limited signal.

3.2. Direction extraction in the different subbands

In order to better extract the local directions present in the image, it is useful to introduce some linear combinations of the primal and dual subbands. To do so, we define the analytic (resp. anti-analytic) wavelets as

$$\psi_m^a(t) = \frac{1}{\sqrt{2}}(\psi_m(t) + \imath\,\psi_m^H(t)), \qquad (13)$$

$$(\text{resp.} \quad \psi_m^{\bar{a}}(t) = \frac{1}{\sqrt{2}}(\psi_m(t) - \imath\,\psi_m^H(t)). \qquad (14)$$

Let us now calculate the tensor product of two analytic wavelets ψ_m^a and $\psi_{m'}^a$. More precisely, we are interested in the real part of this tensor product:

$$\Psi_{m,m'}^a(x,y) = \mathrm{Re}\{\psi_m^a(x)\psi_{m'}^a(y)\}. \qquad (15)$$

For $(m,m') \in \{1,\dots,M-1\}^2$, the Fourier transform of this function is equal to

$$\widehat{\Psi}_{m,m'}^a(\omega_x, \omega_y) =$$
$$\begin{cases} \widehat{\psi}_m(\omega_x)\widehat{\psi}_{m'}(\omega_y) & \text{if } \mathrm{sign}(\omega_x) = \mathrm{sign}(\omega_y), \\ 0 & \text{if } \mathrm{sign}(\omega_x) \neq \mathrm{sign}(\omega_y). \end{cases} \qquad (16)$$

As illustrated in Fig. 1, this function allows us to extract the "directions" falling in the first/third quadrant of the frequency plane. In the same way, the real part of the tensor product of an analytic wavelet and an anti-analytic one is denoted by $\Psi_{m,m'}^{\bar{a}}$. This function allows us to select frequency components which are localized in the second/fourth quadrant of the frequency plane. This corresponds to "opposite" directions to those obtained with $\Psi_{m,m'}^a$.

Fig. 1. 3D Plots of wavelets $\Psi_{2,1}^{\bar{a}}$ (left) and $\Psi_{2,1}^a$ (right).

At a given resolution level j, for each subband (m,m') with $m \neq 0$ and $m' \neq 0$, the directional analysis is achieved by computing the coefficients:

$$d_{j,m,m'}[k,l] = \langle f(x,y), \frac{1}{M^j}\Psi_{m,m'}^{\bar{a}}(\frac{x}{M^j} - k, \frac{y}{M^j} - l)\rangle,$$

$$d_{j,m,m'}^H[k,l] = \langle f(x,y), \frac{1}{M^j}\Psi_{m,m'}^a(\frac{x}{M^j} - k, \frac{y}{M^j} - l)\rangle.$$

According to Eqs. (13), (15), and (14), we have for all $(m,m') \in \{1,\dots,M-1\}^2$,

$$d_{j,m,m'}[k,l] = \frac{1}{\sqrt{2}}(c_{j,m,m'}[k,l] + c_{j,m,m'}^H[k,l]), \qquad (17)$$

$$d_{j,m,m'}^H[k,l] = \frac{1}{\sqrt{2}}(c_{j,m,m'}[k,l] - c_{j,m,m'}^H[k,l]). \qquad (18)$$

Note that Relations (16) is not valid for horizontal or vertical low-pass subbands such that $m = 0$ or $m' = 0$. The corresponding coefficients are left unchanged.

4. OPTIMAL RECONSTRUCTION

Let us denote by $\mathbf{f}$ the vector of image samples. Besides, we denote by $\mathbf{c}$ the vector of coefficients generated by the primal M-band decomposition and by $\mathbf{c}^H$ the vector of coefficients produced by the dual one. The linear combination of the subbands described in Section 3.2 is omitted in the subsequent analysis, since we have seen that this post-processing reduces to a trivial 2×2 isometry. Hence, the global decomposition operator is

$$\mathbf{D}\ :\mathbf{f} \mapsto \begin{pmatrix} \mathbf{c} \\ \mathbf{c}^H \end{pmatrix} = \begin{pmatrix} \mathbf{D_1 f} \\ \mathbf{D_2 f} \end{pmatrix} \qquad (19)$$

where $\mathbf{D_1} = \mathbf{U_1 F_1}$ and $\mathbf{D_2} = \mathbf{U_2 F_2}$, $\mathbf{F_1}$ and $\mathbf{F_2}$ being the pre-filtering operations described in Section 3.1 and $\mathbf{U_1}$ and $\mathbf{U_2}$ being the two considered orthogonal M-band wavelet decompositions. Then, the following results can be proved:

Proposition 2 *Assume that* $(s(x-k, y-l))_{(k,l)\in\mathbb{Z}^2}$ *is an orthonormal family of* $\mathrm{L}^2(\mathbb{R}^2)$. *Provided that there exists* $(A_s, B_s, A_{\psi_0}) \in (\mathbb{R}_+^*)^3$ *such that, for (almost) all* $(\omega_x, \omega_y) \in [-\pi, \pi[^2,$*

$$|\widehat{s}(\omega_x, \omega_y)| \geq A_s, \quad |\widehat{\psi}_0(\omega_x)| \geq A_{\psi_0}$$
$$\sum_{(p,q)\neq(0,0)} |\widehat{s}(\omega_x + 2p\pi, \omega_y + 2q\pi)|^2 \leq B_s < A_s^2 A_{\psi_0}^4$$

$\mathbf{D}$ *is a frame operator. The "dual" frame reconstruction operator*[1] *is given by:*

$$\mathbf{f} = (\mathbf{F_1}^\dagger\mathbf{F_1} + \mathbf{F_2}^\dagger\mathbf{F_2})^{-1}(\mathbf{F_1}^\dagger\mathbf{U_1}^{-1}\mathbf{c} + \mathbf{F_2}^\dagger\mathbf{U_2}^{-1}\mathbf{c}^H), \quad (20)$$

where $\mathbf{T}^\dagger$ *designates the adjoint of an operator* $\mathbf{T}$.

Note that the assumptions on s are obviously satisfied by the Shannon-Nyquist interpolation function. Although other reconstructions of $\mathbf{f}$ from $(\mathbf{c}, \mathbf{c}^H)$ are possible, Formula (20) minimizes the impact of possible errors in the computation of the wavelet coefficients. For example, these errors may arise in the estimation procedures when a denoising application is considered. It is worth pointing out that Eq. (20) is not difficult to implement since $\mathbf{U_1}^{-1}$ and $\mathbf{U_2}^{-1}$ are the inverse M-band wavelet transforms and $\mathbf{F_1}^\dagger$, $\mathbf{F_2}^\dagger$ and $(\mathbf{F_1}^\dagger\mathbf{F_1} + \mathbf{F_2}^\dagger\mathbf{F_2})^{-1}$ correspond to filtering with frequency responses $F_1^*(\omega_x, \omega_y)$, $F_2^*(\omega_x, \omega_y)$ and $(|F_1(\omega_x, \omega_y)|^2 + |F_2(\omega_x, \omega_y)|^2)^{-1}$, respectively.

---

[1]Here "dual" is meant in the sense of the frame theory, which differs from the meaning given in the rest of the paper.

5. APPLICATION TO DENOISING

A denoising example is considered to illustrate the benefit of the proposed decompositions. The 512×512 8-bit Barbara image is corrupted by an additive zero-mean white Gaussian noise which variance is assumed to be known. The noisy image is decomposed via an M-band Discrete Wavelet Transform (DWT) and a Dual-Tree M-band transform (DTT) in the 2, 3 and 4-band cases. For each decomposition, the number of decomposition levels has been fixed so as to get approximation images having roughly the same size at the coarsest resolution. As the filters corresponding to the dual decomposition are not FIR when the filters of the primal decomposition are FIR, frequency domain implementations of the DWT and DTT have been adopted. Different wavelet families have been tested, the provided results corresponding to the use of Meyer's wavelets [18]. The obtained SNR's (in dB) are listed in Tab. 1.

	SURE	NB	Biv	Visu
DWT $M = 2$	11.81	13.11	12.97	8.46
DWT $M = 3$	11.88	13.18	13.04	9.43
DWT $M = 4$	**12.32**	**13.21**	**13.09**	**9.44**
DTT $M = 2$	12.56	13.38	13.46	9.06
DTT $M = 3$	12.62	13.50	13.70	10.17
DTT $M = 4$	**13.06**	**13.60**	**13.88**	**10.53**

Table 1. Denoising results for an initial SNR of 5.2 dB. The considered estimators are SureShrink (SURE) [19]), Neighblock [20] (NB), Bivariate Shrinkage [21] (Biv) and Visushrink (Visu).

First, we observe for this image that, by increasing the number of bands M, the denoising results are improved in all cases both for the DWT and the DTT. Furthermore, the DTT leads to a significant improvement of the denoising performance compared to the DWT.
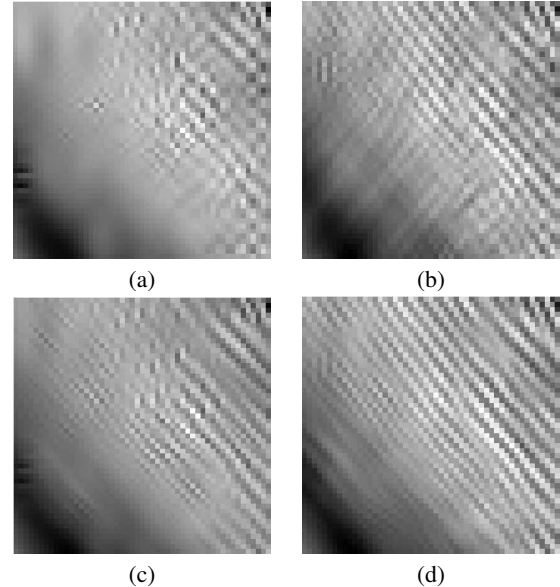
Fig. 2 also illustrates that, compared with other decompositions, the DTT with $M = 4$ leads to sharper visual results and reduced artifacts.

6. CONCLUSIONS

We have shown that M-band dual tree transforms are interesting tools for 2D processing provided that an appropriate pre-filtering is applied, and that some attention is paid to the reconstruction stage. Our experimental results have put emphasis on denoising problems but, due to the directional features which can be obtained with these decompositions, applications to image analysis problems can also be addressed.

(a)   (b)

(c)   (d)

Fig. 2. Denoising results for a cropped version of "Barbara" using Bivariate Shrinkage and: (a) DWT $M = 2$; (b) DWT $M = 4$; (c) DTT $M = 2$; (d) DTT $M = 4$.

7. REFERENCES

[1] Stéphane Mallat, *A wavelet tour of signal processing*, Academic Press, 1998.

[2] J.-C. Pesquet, H. Krim, and H. Carfantan, "Time invariant orthonormal representations," *IEEE Trans. on Signal Proc.*, vol. 44, no. 8, pp. 1964–1970, 1996.

[3] X-P. Zhang, M. Desai, and Y-N. Peng, "Orthogonal complex filter banks and wavelets: some properties and design," *IEEE Trans. on Signal Proc.*, vol. 47, no. 4, pp. 1039–1048, Apr. 1999.

[4] E. P. Simoncelli, W. T. Freeman, E. H. Adelson, and D. J. Heeger, "Shiftable multi-scale transforms," *IEEE Trans. on Inform. Theory*, vol. 38, no. 2, pp. 587–607, March 1992, Special Issue on Wavelets.

[5] N.G. Kingsbury, "Complex wavelets for shift invariant analysis and filtering of signals," *J. of Appl. and Comp. Harm. Analysis*, vol. 10, no. 3, pp. 234–253, May 2001.

[6] P. Abry and P. Flandrin, "Multiresolution transient detection," in *Proc. Int. Symp. on Time-Freq. and Time-Scale Analysis*, 1994, pp. 225–228.

[7] I. W. Selesnick, "Hilbert transform pairs of wavelet bases," *Signal Processing Letters*, vol. 8, no. 6, pp. 170–173, Jun. 2001.

[8] I. W. Selesnick, "The double-density dual-tree DWT," *IEEE Trans. on Signal Proc.*, vol. 52, no. 5, pp. 1304–1314, May 2004.

[9] R. A. Gopinath, "The phaselet transform — an integral redundancy nearly shift-invariant wavelet transform," *IEEE Trans. on Signal Proc.*, pp. 1792– 1805, Jul. 2003.

[10] F. Fernandes, M. Wakin, and R. Baraniuk, "Non-redundant, linear-phase, semi-orthogonal, directional complex wavelets," in *Proc. Int. Conf. on Acoust., Speech and Sig. Proc.*, May 2004.

[11] R. van Spaendonck, T. Blu, R. Baraniuk, and M. Vetterli, "Orthogonal Hilbert transform filter banks and wavelets," in *Proc. Int. Conf. on Acoust., Speech and Sig. Proc.*, 2003, pp. 505–508.

[12] S. C. Olhede and A. T. Walden, "Analytic wavelet thresholding," Tr-03-01, Imperial College, 2003.

[13] W. Chan, H. Choi, and R. Baraniuk, "Directional hypercomplex wavelets for multidimensional signal analysis and processing," in *Proc. Int. Conf. on Acoust., Speech and Sig. Proc.*, May 2004.

[14] Henrique S. Malvar, *Signal Processing with Lapped Transforms*, Artech House, 1992.

[15] P. Steffen, P. N. Heller, R. A. Gopinath, and C. S. Burrus, "Theory of regular M-band wavelet bases," *IEEE Trans. on Signal Proc.*, vol. 41, no. 12, pp. 3497–3511, Dec. 1993.

[16] T. D. Tran, R. L. de Queiroz, and T. Q. Nguyen, "Linear phase perfect reconstruction filter bank: lattice structure, design, and application in image coding," *IEEE Trans. on Signal Proc.*, vol. 48, pp. 133–147, Jan. 2000.

[17] C. Chaux, L. Duval, and J.-C. Pesquet, "Hilbert pairs of M-band orthonormal wavelet bases," in *Proc. European Signal Processing Conference (EUSIPCO)*, pp. 1187–1190.

[18] B. Tennant and R. M. Rao, "Solution to the orthogonal M-channel bandlimited wavelet construction proposition," in *Proc. Int. Conf. on Acoust., Speech and Sig. Proc.*, 2003.

[19] D. L. Donoho and I. M. Johnstone, "Adapting to unknown smoothness via wavelet shrinkage," *Journal of the American Statistical Association*, vol. 90, pp. 1200–1224, December 1995.

[20] T. T. Cai and B. W. Silverman, "Incorporating information on neighboring coefficients into wavelet estimation," *Sankhya*, vol. 63, pp. 127–148, 2001.

[21] L. Sendur and I. W. Selesnick, "Bivariate shrinkage with local variance estimation," *Signal Processing Letters*, vol. 9, no. 12, pp. 438–441, Dec. 2002.